Potassic late orogenic Stephanian volcanism in the South West french Massif Central (Decazeville, Figeac, Lacapelle-Marival basins): an example for mantle metasomatism along strike-slip faults?

Henriette Lapierre, Christophe Basile, Thomas Berly, Emmanuel Canard

Potassic late orogenic Stephanian volcanism in the South West french Massif Central (Decazeville, Figeac, Lacapelle-Marival basins): an example for mantle metasomatism along strike-slip faults?

H. Lapierre[†], C. Basile[*], T. Berly, E. Canard

Laboratoire de Géodynamique des Chaînes Alpines, CNRS UMR 5025, Observatoire des Sciences de l'Univers de Grenoble, Université Joseph Fourier. Maison des Géosciences, 1381 rue de la Piscine, 38400 St Martin d'Hères, France.

† Deceased in January 2006

* Corresponding author cbasile@ujf-grenoble.fr

Keywords: late orogenic magmatism, shoshonitic, Sillon Houiller fault, Variscan

***Mots clefs**: magmatisme tardi-orogénique, shoshonitique, Sillon Houiller, Varisque*

Abstract

In the Southwestern french Massif Central (Decazeville basin, at the Sillon Houiller fault termination; Figeac and Lacapelle-Marival basins along Argentat fault) the Stephanian volcanism exhibit homogeous geochemical features. This magmatism has shoshonitic affinities. Their chondrite-normalized Rare Earth Element (REE) spectra are enriched in light REE, but almost flat for heavy REE, with a marked negative Eu anomaly. Primitive mantle-normalized element spectra show negative Nb, Ta, P, Sm, Ti, and positive Th, U, Pb anomalies, respectively. ε_{Nd} values are negative and also homogeneous (between -6 and -4). This volcanism share the same geochemical patterns with the late-orogenic Stephanian-Permian magmatism from the southern part of the Variscan belt (Pyrénées, Alps, Sardinia).

We interpret these characteristics as resulting from the partial melt of a metasomatism mantle. We propose a new mechanism to explain this melt: horizontal displacement along the mainlate-orogenic strike-slip fault may bring into contact an hydrated lower crust with the lithospheric mantle. Mantle metasomatism within the strike-slip fault zone may then induce partial melting.

Résumé

Le volcanisme Stéphanien du Sud Ouest du Massif Central français (bassins de Decazeville à l'extrémité du Sillon Houiller, de Figeac et Lacapelle-Marival le long de la faille d'Argentat) présente des caractéristiques géochimiques homogènes. Il s'agit d'un magmatisme d'affinité shoshonitique, présentant des spectres de terres rares normalisés aux chondrites enrichis en terre rares légères, mais presque plat pour les terres rares lourdes, avec une anomalie négative en Eu marquée. Les spectres élémentaires normalisés au manteau primitif montrent des anomalies négatives en Nb, Ta, P, Sm et Ti, et des anomalies positives en Th, U et Pb. Les valeurs d'ε_{Nd} sont négatives et également très homogènes (-6 à -4). Ce volcanisme présente les mêmes caractéristiques que le volcanisme tardi-orogénique stéphano-permien du Sud de la chaîne varisque (Pyrénées, Alpes, Sardaigne). Ces caractéristiques sont interprétées comme résultant de la fusion partielle d'une source mantellique métasomatisée. Il est proposé un nouveau mécanisme provoquant cette fusion, par l'intermédiaire du déplacement horizontal des failles décrochantes tardi-orogéniques majeures, qui pourrait mettre en contact une croûte inférieure hydratée et le manteau lithosphérique. Le métasomatisme du manteau à l'intérieur de la zone de faille décrochante provoquerait sa fusion.

Introduction

Late orogenic times represent a key period of mountain belt evolution, when the continental lithosphere acquires a new structure that will control further evolution, including its remobilization in new orogenes. The continental crust is particularly modified by late orogenic magmatism and tectonism. Bimodal magmatism is widespread, and results mainly from crustal melting, and partly from mantle partial melting (Bonin, 2004). The magmas evolving from mantle melts are commonly Potassium-rich (High Potassium Calc Alcaline: HKCA, e.g. Liégeois et al., 1998), but the mechanisms associated with this enrichment are still a matter of discussion. This magmatism is coeval with a change in the tectonic regime, from regional compression to strike-slip, then extensional regime, that precedes the tectonic quiescence (e.g. Blès et al., 1989). The strike-slip regime generates numerous vertical faults that cross-cut the orogenic structures.

At the end of the Variscan orogeny, Westphalian synkinematic plutonism accommodated extension parallel to the mountain belt (Faure, 1995). Before the post-orogenic Permian widespread extension, Stephanian represents a transition with numerous strike-slip faults associated with intracontinental coal-bearing basins. In the french Massif Central, the Sillon Houiller is one of these strike-slip faults (Figure 1), coeval with the formation of numerous deep and narrow Stephanian basins first infilled by potassic volcanism (Letourneur, 1953). Similar potassic volcanism is also known in other Stephanian basins, for example along the Argentat normal fault in the western part of the Massif Central (Figure 1). These two faults meet in the southwestern Massif Central, where a direct comparison of late orogenic potassic volcanism can be performed in coeval strike-slip and extensional basins.

Geological setting

The present study focus on the volcanism located in the Decazeville basin, at the southern termination of the Sillon Houiller, and in Figeac and Lacapelle-Marival basins along the Argentat fault.

The Sillon houiller fault is a 270 km-long, nearly N-S striking left-lateral fault, that crosses the entire Massif Central (Figure 1). The cumulated horizontal displacement has been estimated to be less than one hundred kilometers (Grolier and Letourneur, 1968). This fault has been considered as a transfer fault accommodating differences in the directions of extension (Namurian and early Stephanian, Burg et al., 1990) or in the amount of extension (Stephanian and Autunian, Faure, 1995). More recently, Basile (2006) proposed that it was a transform fault during Stephanian times, and that Decazeville basin was tectonically controled by its horsetail splay termination in a transtensional regime. In the lowermost part of the basin infilling, a thick volcanic complex lies on a coarse conglomerate (Figure 1). The upper part of the 1800 m-thick sedimentary section is devoid of volcanism, with the possible exception of few thin layers of tuffs intercalated in lacustrine to deltaic continental sediments.

The Argentat fault is a 160 km-long curved fault in the western part of the Massif Central, from the Bosmoreau Carboniferous basin in the north to the Decazeville basin in the south (Figure 1). This fault strikes N-S in its northern part, and NW-SE in its southern part. The Argentat fault was first a right-lateral ductile normal fault, then a brittle strike-slip fault during the late Carboniferous (Feix et al., 1987; Roig et al., 1997). Figeac, St Perdoux and Lacapelle-Marival represent the southernmost basins associated to this fault (Figure 1). They are not directly bounded by the Argentat fault, but appear as the Argentat basin located on a basement flexure (Genna et al., 1998). Because of Mesozoic sedimentary cover, the connection between Figeac and Lacapelle-Marival basins is actually hidden (Figure 1), but they certainly belong to a single basin whose remnants were also found in drilled holes below the Mesozoic

sediments (Lefavrais-Raymond et al., 1990). As in Decazeville basin, the 300 to 400 m-thick volcanic complex is located at the base of the basin infilling, overlain by coarse detrital sediments. Numerous NW-SE-trending feeding dikes also cross the basement near Lacapelle-Marival basin (Figure 1), indicating in this area a NE-SW extension during volcanism and basin subsidence.

In these basins, the sediments are middle Stephanian (Stephanian B) in age, with early Stephanian (A) suspected in the St Perdoux basin, and the base of late Stephanian (C) observed in the Decazeville basin (Figure 1) (Vetter, 1968). Permian sediments unconformably cover the eastern part of Decazeville basin, and were also found in Figeac basin (Lefavrais-Raymond et al., 1990). The age of volcanism is also assummed to be Stephanian, but may be controversial in the Decazeville basin: from palynology, the older sediments were dated from the base of middle Stephanian (Vetter, 1968), whereas U-Pb dating on unlocated volcanic zircons provided an older age (Visean: 333 Ma) (Bruguier et al., 1998).

Volcanism consist either in basalts or trachytes and rhyolites, mainly as flows, but also as ejecta and numerous dikes in the crystalline basement. Morre (1966) and Morre and Quesnel (1967) emphasized on the Potassium-rich character of these lava, especially in trachytes where K_2O ranges from 6 to 11%.

- North of Decazeville basin, the samples were collected from two areas (Figure 1), the Bouran section along the D963 road (samples CLB95-1 to –8), and the Lot banks on each side of Livinhac bridge (CLB95-9 to –17, and CLB96-1). The Bourran section consists of volcaniclastic rocks and volcanic flows conformably overlain by detritic sediments (Campagnac unit, Vetter, 1968). The graded bedded volcaniclastic rocks rest unconformably on Variscan micaschists, and consist of breccias and lapilli-tuffs, interlayered with massive volcanic flows. The breccias are composed of meter-sized rounded volcanic blocks caught in

a tuffaceous matrix while the lapilli-tuffs include centimeter-sized angular volcanic fragments. The lapilli-tuffs locally grade to millimeter-sized crystal tuffs. Near Livinhac, massive basalts are exposed on both sides of the Lot river. The northern outcrop is cross-cutted by a monzo-diorite porphyric dike (CLB95-17).

- In Figeac area, we sampled two sections, East (Célé river blank, samples CLB96-5) and North (along Planioles creek, samples CLB96-2 and -3) of Figeac city, respectively (Figure 1). Along the Planioles section, hyalopilitic basalts crop out overlain successively by vitric tuffs, very altered rhyolites and detritic sediments. Two massive trachytic flows outcrop in the Célé valley.

- Near Lacapelle-Marival, two volcanic levels are interbedded with Carboniferous shales, sandstones and conglomerates. Sampling (CLB96-13 to -17) in the northern part of the basin (massive basalt flows), and southward (CLB96-6 to -12) in small outcrops of trachytes and rhyolites (Figure 1).

Petrology and mineralogy

The studied volcanic rocks are more or less intensely altered. Plagioclase is often replaced by albite or sericite or even quartz and epidote. Olivine is altered into iddingsite, serpentine or smectites. Orthopyroxene and clinopyroxene remain most commonly fresh. Biotite and hornblende are often chloritized. When altered, alkali feldspar is replaced by orthose or albite. Ti-rich oxides are replaced by titanite. Mafic glass has crystallized into chlorite ± smectites with frequent calcite or smectites-filled vesicules while the groundmass of the trachytes and rhyolites consists of fine grained quartz associated sometimes with alkali feldspar (albite or adularia). As no metamorphism has been observed in the Stephanian (or younger) sediments, the occurence of chlorite probably indicates hydrothermal alteration.

Despite this weathering, the following characteristic can be observed: in both Decazeville and Lacapelle-Marival basins, most mafic rocks are glomero-porphyritic with clots of large zoned plagioclase, orthopyroxene and clinopyroxene phenocrysts associated either with olivine or amphibole and biotite ± quartz. The groundmass includes plagioclase microlites and oxydes. Quartz xenocrysts rimmed by orthopyroxene may occur. In Lacapelle-Marival area, some basalts differ by the presence of trachytoid texture formed of plagioclase laths (30 %) and less abundant and large phenocrysts (~ 10 %). The trachytes exhibit seriate textures with millemeter-sized alkali feldspar phenocrysts. Their groundmass includes sandstone inclusions and quartz-filled flattenned vesicles. The rhyolites exhibit quartz and feldspar phenocrysts (20 %) and biotite needles (~ 10 %), that includes apatite and zircon. The Figeac rhyolites differ from those from Lacapelle Marival by the presence of green hornblende.

When preserved (CLB95-5, CLB95-16, CLB96-1, CLB96-3), plagioclase composition of mafic volcanic rocks varies from Ca-rich cores (An_{98-60}) to Na-enriched rims (An_{50-40}). Preserved alkali feldspar in the trachytes (CLB96-11) displays a sanidine composition (Ab_{57-66}). Clinopyroxene phenocrysts (CLB96-1, CLB95-16, CLB95-5) have very homogeneous compositions which are those of augite (Wo_{39-44} En_{44-52} Fs_{12-21}; Morimoto et al. 1988). Preserved orthopyroxene (CLB95-5, CLB95-16) has a clinoenstatite composition ($Wo_{2-2.5}$ En_{77-78} Fs_{19-21}).

Analytical techniques

Thirty one samples have been analyzed for whole rock major, trace element, and Nd and Sr isotopic chemistry (Table 1). Major and compatible trace elements have been measured by ICP-AES at the Centre de Recherches Pétrographiques et Géochimiques de Nancy (samples CLB95) or by X-ray fluorescence (XRF) at the Earth Sciences Department of the Australian

National University at Canberra (Australia) (samples CLB96). The trace elements have been determined by inductively coupled plasma mass spectrometry (ICP-MS, VG-PQ^{2+}) at the Laboratoire de Géodynamique des Chaînes Alpines de l'Université Joseph Fourier (Grenoble), after acid dissolution, using procedures of Barrat et al. (1996). Standards used for the analyses were JB2, WSE, BIR-1, JR1, and BHVO.

Sr and Nd isotopic ratios were measured at the Laboratoire de Géochimie isotopique de l'Université Paul Sabatier de Toulouse on a Finnigan MAT261 multicollector mass spectrometer using the analytical procedures of Lapierre et al. (1997). Results on La Jolla Nd standards yielded $^{143}Nd/^{144}Nd = 0.511850 \pm 8$ (mean on 39 runs). Results on NBS 987 Sr standard yielded $^{87}Sr/^{86}Sr = 0.710250 \pm 5$ (mean on 200 runs). The isotopic data have been corrected for “in situ decay” with age of 300 Ma.

Alteration and elemental mobility

The altered nature (up to low grade greenschist facies) of the studied Carboniferous volcanic rocks means that before any petrological inferences can be drawn from the chemistry of the rocks, the possible chemical effects of subsolidus of elements must be accounted for. Most of the analyzed rocks have a loss of ignition lower than 6% (Table 1), due to the presence of calcite- or smectites-filled vesicules.

Zirconium (Zr) is considered as being immobile during low grade alteration of igneous rocks of mafic to felsic composition by hydrothermal fluids (Gibson et al., 1982) and so has been plotted against minor (TiO_2), and incompatible trace elements (Rb, Sr, Pb, La, Nb, Y, U and Th) in Figure 2. Rb, Sr, Pb and La display no correlation with Zr. This implies that the large ion lithophile elements have been extensively mobilised. For example, some samples are enriched in Pb (others in Ba), probably in relation with hydrothermal circulations (Marignac

and Cuney, 1999). Thus, variations in these large ion lithophile elements are not expected to reflect the compositions of the sources (Sr isotopic ratios) or magmatic processes. These variations will not be discussed further on. Similar behaviour for K and Ca exclude their use for sample classification.

In contrast, other elements like U, Th, Nb or TiO_2 correlate rather well with Zr, implying relative immobility. However, some samples (CLB95-17, 95-15, 95-1, 96-5) separate from the correlation trend between Nb and Zr. The same samples define a TiO2-Zr negative correlation, while most other samples exhibit a positive correlation. In Y-Zr diagram, each site corresponds to a distinct Y-Zr correlation. These various trends suggest that the Carboniferous volcanic rocks are not linked together by simple fractionation process. The various Y versus Zr correlations may reflect variation of partial melting ratios, and/or complex fractionation process dominated by clinopyroxene or amphibole accumulation and/or removal.

Volcanic rocks terminology

Because of the alteration experienced by the Carboniferous volcanic rocks, it was difficult to name the different facies on the only basis of mineralogy, especially for the mafic rocks. In the following sections, we use three rock types based on the MgO contents of the rocks: basalts (MgO $\geq$ 5%), trachy-andesites (2 < MgO < 5 %), and rhyolites (MgO $\leq$ 2%) (Table 1). Because MgO and SiO2 are very well correlated for each Decazeville and Figeac sites (Figure 3), these rock types are consistent with those defined by SiO2 contents. In contrast MgO and SiO2 are poorly or not correlated in Lacapelle-Marival sites (Figure 3), where naming can be ambiguous for some samples.

In a Zr/Ti versus Nb/Y diagram (Figure 4, Winchester and Floyd, 1977), basalts and most trachy-andesites plot near the fence separating the field of rhyodacites from that of andesites with the exception of the most Mg-rich Decazeville basalt (CLB95-17) which falls in the andesite and basalt field. Basalts (except CLB95-17) and trachy-andesites have similar Zr/Ti ratio but differ on the Nb/Y ratio. Most rhyolites plot in the rhyodacite-dacite field, some in the rhyolite, trachyte or trachy-andesite fields. While SiO2- and Zr-rich, they are relativeley Ti-poor (Figure 2), and define a distinct group from the trachy-andesites. It is noteworthy that the basalts plot at the intersection of the two groups. The discrepancies between the terminologies based on the MgO content and incompatible trace element ratios can be attributed to the specific geochemical features of these rocks which display alltogether sub-alkaline and alkaline features, like all the K-rich suites.

Because of the well known K mobility during alteration and low grade metamorphism processes, we cannot rely on the K contents of the Carboniferous volcanic rocks (half of the samples have K contents from 6 to 12%) to infer their calc-alkaline or shoshonitic affinity. Therefore, we plotted the rocks on the Th/Yb versus Ta/Yb correlation diagrams used to discriminate arc-tholeiites, calc-alkaline and shoshonitic suites (Figure 5, Müller et al., 1992). Most of the Carboniferous volcanic rocks fall in the shoshonitic field with the exception of 95-17 basalt which show calc-alkaline affinities. In this plot as previously observed, basalts and trachy-andesites positions do not differ. The rhyolites exhibit a more shoshonitic affinity.

Trace-element geochemistry

Figure 6 illustrates the chondrite-normalized (Sun and McDonough, 1989) Rare Earth Elements (REE) patterns of the Carboniferous volcanic rocks. All the rocks are enriched in Light (L) REE relative to the heavy (H) REE [$31.9 \leq (La/Yb)_n \leq 2.8$]. However, HREE

pattern is either flat or gently sloping, suggesting that LREE enrichment reflects a metasomatised source. All samples also show marked negative Eu anomalies ($0.84 < Eu/Eu^* < 0.38$), especially in trachy-andesites and rhyolites. These anomalies suggest an early fractionation of plagioclase during magma differentiation. Rhyolites and some trachy-andesites are less enriched than basalts, especially for HREE. This indicates again that these lavas can not result from fractional crystallisation of basalts.

There is no significative differences between the sampling sites, with the exception of a negative Ce anomalies ($0.67 \leq Ce/Ce^* \leq 0.38$) for four trachy-andesites from the southern part of Lacapelle-Marival basin (CLB96-6, CLB96-10 to -12). Two trachy-andesites from Decazeville (CLB95-8, CLB95-9) differ from the other rocks by flatter patterns [$4.9 < (La/Yb)_n < 2.8$]. The alkaline rhyolite from Livinhac site (CLB95-15) differs from the other felsic rocks by a very steep pattern due to an important HREE depletion [$(La/Yb)_n = 31.9$].

Figure 7 shows the primitive mantle-normalized spiderdiagrams (Sun and McDonough, 1989). Whatever their location or mafic character, Carboniferous volcanic rocks exhibit similar trace element compositions. They are characterized by negative Nb, Ta, P, Sm, Ti and positive Th, U and Pb anomalies, respectively. As shown previously (Figure 2), Sr contents vary within a wide range, especially in rhyolites and trachy-andesites. More generally, basalts exhibit an homogeneous composition for all trace elements, with the exception of CLB95-17 that differs from the other mafic rocks by a Zr and Hf depletion. CLB95-17 as other samples (CLB95-1, 95-13, 95-15, 96-5) that define a negative correlation in TiO2/Zr correlation (Figure 2) are all characterized by a negative Y anomaly. Finally, the Decazeville (Bourran, Livinhac) trachy-andesites differ from those of Figeac and Lacapelle-Marival by higher Pb abundances.

Nd and Sr sotopic geochemistry

The Carboniferous volcanic rocks span a rather small range of ε_{Nd} values, from -5.8 to -3.9, with the relative exception of CLB96-5 rhyolite (ε_{Nd} = -2.2). All ε_{Nd} are negative, and do not present significative variations with petrography, rock type or rock chemistry (Table 1). These very homogeneous values suggest a cogenetic link between these lavas, and indicate a crustal signature. The $^{87}Sr/^{86}Sr$ ratio is less homogeneous and ranges between 0.71128 and 0.70415; ε_{Sr} ranges from 0 to 325 (Table 1). As exposed above, Rb and Sr mobility during hydrothermalism and alteration precludes any use of these elements as markers of the magmatic sources.

Discussion

- Geochemistry

Whatever their location or petrology, all the analysed samples share in common high $(La/Yb)_n$ ratios but almost flat HREE patterns, marked negative Eu anomalies, homogeneous negative ε_{Nd} values (between –6 and –4) and in primitive mantle-normalized plots, negative Nb, Ta, P, Sm, Ti anomalies and positive Th, U and Pb anomalies. Most rhyolites (defined by MgO < 2%) and one basalt (CLB95-17) can be distinguished from other samples by a negative correlation in Ti/Zr diagrams (Figures 2 and 4). These samples present additional geochemical characteristics, such as Y depletion and enhanced negative Ti anomalies, and for some samples negative Ce anomalies.

As rhyolites and most trachy-andesites display REE spectrum less enriched in LREE than basalts, these rocks can not be linked only by crystal fractionation and differentiation. However, as they present similar characteristics, all these lavas may have been formed from similar sources and by similar mechanisms. The occurence of mafic rocks implies mantle

partial melting. All these rocks belong to a shoshonitic suite, characterized by the absence of Ti and Fe enrichment during crystal fractionation. This is a classical feature of hydrous melts (Gill, 1981).

As examplified by the occurence of sedimentary xenoliths in these lavas, subsequent contamination of magmas likely occurred. Nb and Ta negative anomalies in primitive-normalized plots are independent of their magmatic affinities. This suggest that the lower continental crust, known to be depleted in Nb and Ta, is involved in the genesis of these rocks, even for the more mafic. Similarly, U and Th may be explained by contamination by continental crust, while the negative Ce anomaly may indicate contamination by oceanic rocks (sediments or altered oceanic crust). These contaminations may occur either during the rising of magma, but more probably reflect the direct contribution of hydrous crustal materials to mantle melting, as suggested by the negative ε_{Nd} values, the homogeneous shape of REE patterns, and the Ti/Y versus Zr/Y and Nb/La versus Th/La diagrams (Figure 8). All rocks but one basalt (CLB95-17) in both diagrams and rhyolites in Ti/Y versus Zr/Y diagram display a positive linear trend. This suggests that the contamination by crustal material is strictly linked to the source melting, i.e. that the melting protolith was a mix of mantle and crustal materials. Among the analyzed rocks, the Decazeville trachy-andesites have the highest Ti/Y, Zr/Y, Nb/La and Th/La ratios, suggesting that the proportion of crutal material was higher in the source of these volcanic rocks.

Initial fractionation of apatite from these melts can explain P negative anomalies. Similarly, the negative anomalies in Ti, Eu and Y can be explained by early fractionation of Fe-Ti oxydes (sometimes found included in phenocrysts), plagioclases and clinopyroxenes, respectively. The peculiar Y depletion of rhyolites and CLB95-17 basalt can be explained by clinopyroxene or amphibole fractionation, that may have not occur for the other lavas. Similarly, there negative Ti/Zr correlation can indicate Fe-Ti oxydes fractionation.

- Structural control on magmatism

Despite the difference in the structural setting, there is no difference in the petrology or geochemistry between Decazeville, Figeac and Lacapelle-Marival basins. The surface faults and the tectonic regime control the formation of Stephanian basins, where the volcanism took place, but they do not influence its petrology or geochemistry. The NW-SE striking dykes in the basement of Lacapelle-Marival basin, and the occurence of volcanism as the first infilling of all the basins along the Sillon Houiller fault indicate a strike-slip tectonic regime at the french Massif Central scale, with NE-SW stretching direction and NW-SE shortening direction. This regime is associated to the left-lateral slip on the Sillon Houiller fault, and to extension or right-lateral transtension along the Argentat fault. It seems to be the main tectonic regime at the time of the infilling of the Stephanian basins along these faults (Basile, 2006). As the same volcanism systematically occurred in all the basins along the Sillon Houiller fault (Letourneur, 1953), it can be proposed that the Lacapelle-Marival volcanism, located only 25 km West of the Sillon Houiller fault, came from the same source as for the Decazeville volcanism. The local difference in the tectonic regime only controlled the volume and surface covered by volcanic flows.

- Late-orogenic Variscan magmatism

The Stephanian volcanism from the french Massif Central belongs to the large K-rich igneous province emplaced during Stephanian to Early Permian times in the southern part of the european Variscan belt (Pyrénées: Innocent et al., 1994; Western Alps: Cannic et al., 2002; Central Alps: Schaltegger et al., 1991; Southern Alps: Rottura et al., 1998, Cortesogno et al., 1998; Corsica and Sardinia: Tommasini et al., 1995). In the Pyrénées (Bixel and Lucas, 1983) and Western Alps (Capuzzo and Bussy, 2000), this volcanism is located in basins

clearly controlled by strike-slip faults. Together with the K-rich character, this igneous province share similar geochemical patterns with the Stephanian volcanism for the SW Massif Central: in chondrite-normalized diagrams, LREE-enriched patterns, flat HREE spectrum and negative Eu anomaly; in primitive mantle normalized diagrams, negative Nb, Ta and Ti anomalies, and postive Th and U anomalies; and negative ε_{Nd} values (-3 to -7), with the exception of the most recent (Permian) lava that have slightly positive ε_{Nd} values. It is noteworthy that these geochemical characteristics were homegeneous during a large time span and in various parts of the Variscan belt. If the position of alpine massifs in the Variscan belt can be a matter of debate, similar volcanism occurred in the Massif Central (internal zones) and in the Pyrénées (external zone within the subducting plate).

- Geodynamical implications

The origin of potassic late-orogenic magmatismhas beenand is still a matter of debate. As this magmatism indicates an hydrous melting, some authors (e.g. Stampfli, 1996) proposed that it generated insubduction or back-arc setting. However, in the studied example, the late-orogenic timing as the position within the subducting plate are not in favour of this hypothesis. More frequently, the geochemical patterns have been explained by contamination, either by mantle metasomatism before melting, or by crustal contamination during magma ascent. However, the systematic and homogeneous character of contamination suggests as in this study that the mantle source was contaminated before melting. This metasomatism may result from variscan or previous subductions, depending on the position in the variscan belt.

The main mechanism used to explain the metasomatised mantle melt is the post-orogenic lithospheric extension and induced mantle decompression (e.g. Innocent et al., 1994; Rottura et al., 1998). However, the Stephanian volcanism occurred in a strike-slip tectonic regime in

the french Massif Central, and significatively before the main Permian extension that ended the variscan orogenic cycle (Ménard and Molnar, 1988).

We can propose an alternative mechanism, controlled by strike-slip faulting, to explain the potassic late-variscan volcanism whatever the location in the mountain belt. At the end of the orogeny, the various parts of the mountain belt differ by their crustal and lithospheric thicknesses, thermal gradients, nature and history. As the late-orogenic strike-slip faults cross the orogenic zonation withsome tens or hundreds kilometers horizontal slips, they bring into contact different parts of the mountain belt. For example, the horizontal displacement of a thick block from the internal to the external zone may bring into contact the lower crust from the internal zone with the lithospheric mantle of the external zone. The crustal fluids then hydrate the adjacent mantle, and this metasomatism induces mantle melting. The resulting magmas have geochemical patterns that indicate contamination by continental crust. In this hypothetical mechanism, mantle melting is not initiated by vertical but horizontal displacements. Mantle metasomatism then does not required to be previously acquired, but directly induce mantle melting within the strike-slip fault zone, and produce magmatic series which share many petrological and geochemical patterns with arc magmatism.

Acknowledgements

D. Arnaud, F. Senebier and F. Coeur are thanked for sampling preparation, F. Keller and L. Briqueu for the chemical analyses, F. Chauvet for helpfull discussions. This work has been funded by the LGCA.

References

BARRAT J.A., KELLER F., AMOSSE J., TAYLOR R.N., NESBITT R.W. & HIRATA T. (1996).- Determination of rare earth elements in sixteen silicate reference samples by ICP-MS after Tm addition and ion exchange separation.- *Geost. Newsletter*, **32**, 133-139.

BASILE C. (2006).- A new interpretation of Stephanian deformation in the Decazeville basin (Massif Central, France): consequences on late Variscan tectonism.- *Int. J. Earth Sci.*, **95**, 5, 791-801.

BIXEL F. & LUCAS C. (1983).- Magmatisme, tectonique et sédimentation dans les fossés stéphano-permiens des Pyrénées occidentales.- *Rev. Geol. Dyn. Geogr. Phys.*, **24**, 4, 329-342.

BLES J.L., BONIJOLY D., CASTAING C. & GROS Y. (1989).- Successive post-Variscan stress fields in the French Massif Central and its border (Western European plate) : comparison with geodynamic data.- *Tectonophysics*, **169**, 79-111.

BONIN B. (2004).- Do coeval mafic and felsic magmas in post-collisional to within-plate regimes necessarily imply two constrasting, mantle and crustal, sources? A review.- *Lithos*, **78**, 1-24.

BRUGUIER O., BECQ-GIRAUDON J.F., BOSCH D. & LANCELOT J.R. (1998).- Late Visean hidden basins in the internal zones of the variscan belt: U-Pb zircon evidence from the French Massif Central.- *Geology*, **26**, 627-630.

BURG J., BRUN J.P. & VAN DEN DRIESSCHE J. (1990).- Le Sillon houiller du Massif Central français: faille de transfert pendant l'amincissement crustal de la chaîne varisque?- *C. R. Acad. Sci. Paris*, **311**, 147-152.

CANNIC S., LAPIERRE H., MONIE P., BRIQUEU L. & BASILE C. (2002).- Late orogenic evolution of the Variscan lithosphere: Nd isotopic constraints from the western Alps.- *Schweiz. Mineral. Petrogr. Mitt.*, **82**, 77-99.

CAPUZZO N. & BUSSY F. (2000).- High-precision dating and origin of synsedimentary volcanism in the Late Carboniferous Salvan-Dorenaz basin (Aiguilles Rouges Massif, Western Alps).- *Schweiz. Mineral. Petrogr. Mitt.*, **80**, 147-167.

CORTESOGNO L., CASSINIS G., DALLAGIOVANNA G., GAGGERO L., OGGIANO G., RONCHI A., SENO S. & VANOSSI M. (1998).- The Variscan post-collisional volcanism in Late Carboniferous-Permian sequences of Ligurian Alps, Southern Alps and Sardinia (Italy): a synthesis.- *Lithos*, **45**, 305-328.

FAURE M. (1995).- Late orogenic carboniferous extensions in the Variscan French Massif Central.- *Tectonics*, **14**, 132-153.

FEIX I., GUILLOT P.L., MIYASHITA S., BOSSIERE G. & FLOC'H J.P. (1987).- Arguments en faveur d'un épisode majeur en cisaillement dextre le long de la faille d'Argentat (Massif Central). Conséquences.- *C. R. Acad. Sci. Paris*, **305**, 473-476.

GENNA A., ROIG J.Y., DEBRIETTE P.J. & BOUCHOT V. (1998).- Le bassin houiller d'Argentat (Massif Central français), conséquence topographique d'un plissement de son substratum varisque.- *C. R. Acad. Sci. Paris*, **327**, 279-284.

GIBSON I.L., KIRKPATRICK R.J., EMMERMANN R., SCHMINCKE H.U., PRITCHARD G., OAKLEY P.J., THORPE R.S. & MARRINER G.F. (1982).- The trace-element composition of the lavas and dikes from a 3-km vertical section through the lava pile of eastern Iceland.- *J. Geophys. Res.*, **87**, 6532-6546.

GILL J. (1981).- Orogenic andesites and plate tectonics.- Springer-Verlag, New York, 390 p.

GROLIER J. & LETOURNEUR J. (1968).- L'évolution tectonique du grand Sillon houiller du Massif Central français.- XXIII^{ème} Congrès Géologique International, **1**, 107-116.

INNOCENT C., BRIQUEU L. & CABANIS B. (1994).- Sr-Nd isotope and trace-element geochemistry of late Variscan volcanism in the Pyrénées: magmatism in post-orogenic extension?- *Tectonophysics,* **238** 161-181.

LAPIERRE H., DUPUIS V., DE LEPINAY B.M., TARDY M., RUIZ J., MAURY R.C., HERNANDEZ J. & LOUBET M. (1997).- Is the lower Duarte Igneous Complex (Hispaniola) a remnant of the Caribbean plume-generated oceanic plateau?- *J. Geol.,* **105**, 1, 111-120.

LEFAVRAIS-RAYMOND A., ASTRUC J.G., GUILLOT P.L., BONIJOLY D., LEFAVRAIS-HENRY M. & MARANDAT B. (1990).- Notice explicative, Carte géol. France (1/50 000), feuille Figeac (858).- Orléans, Bureau de Recherches Géologiques et Minières, 92 p.

LETOURNEUR J. (1953).- Le grand Sillon houiller du Plateau Central français.- *Bull. Serv. Carte Géologique de la France*, **51**, 1-236.

LIEGEOIS J.P., NAVEZ J., HERTOGEN J. & BLACK R. (1998).- Constrasting origin of post-collisional high-K calc-alkaline and shoshonitic versus alkaline and peralkaline granitoids. The use of sliding normalization.- *Lithos*, **45**, 1-28.

MARIGNAC C. & CUNEY M. (1999).- Ore deposits of the French Massif Central: insight into the metallogenesis of the Variscan collision belt.- *Min. Depos.*, 34, 472-504.

MENARD G. & MOLNAR P. (1988).- Collapse of a Hercynian Tibetan plateau into a late Paleozoic European basin and range province.- *Nature,* **334**, 235-237.

MORIMOTO N., FABRIES J., FERGUSON A.K., GINZBURG I.V., ROSS M., SEIFERT F.A, ZUSSMAN J., AOKI K. & GOTTARDI G. (1988).- Nomenclature of pyroxenes.- *Am. Min.,* **73**, 9-10, 1123-1133.

MORRE N. (1966).- Etude pétrographique sur les roches volcaniques carbonifères de la région de Figeac.- *Bull. Soc. Geol. Fr.,* **7**, 8, 2, 322-328.

MORRE N. & QUESNEL G. (1967).- Etude pétrographique sur les roches volcaniques carbonifères de Lacapelle-Marival.- *C. R. Somm. Soc. Géol. Fr.*, **4**, 160-161.

MÜLLER D., ROCK N.M.S & GROVES D.I. (1992).- Geochemical discrimination between shoshonitic and potassic volcanic rocks in different tectonic settings: a pilot study.- *Mineral. Petrol.*, **46**, 259-289.

ROIG J.Y., CALCAGNO P., BOUCHOT V., MALUSKI H. & FAURE M. (1997).- Modélisation 3D du paléochamp hydrothermal As + Au (330-300 Ma) le long de la faille d'Argentat (Massif Central français).- *Chron. Rech. Min.*, **528**, 63-69.

ROTTURA A., BARGOSSI G.M., CAGGIANELLI A., DEL MORO A., VISONA D. & TRANNE C.A. (1998).- Origin and significance of the Permian high-K calc-alkaline magmatism in the central-eastern Southern Alps, Italy.- *Lithos*, **45**, 329-348.

SCHALTEGGER U., GNOS E., KÜPFER T. & LABHART T.P. (1991).- Geochemistry and tectonic significance of Late Hercynian potassic and ultrapotassic magmatism in the Aar massif (Central Alps).- *Schweiz. Mineral. Petrogr. Mitt.*, **71**, 391-403.

STAMPFLI G. (1996).- The Intra-Alpaine terrain: a paleo-tethyan remnant in the Alpine Variscides.- *Eclogae Geol. Helv.*, **89**, 13-42.

SUN S.S. & MCDONOUGH W.F. (1989).- Chemical and isotopic systematics of oceanic basalts: implications for mantle composition and processes.- *Geol. Soc. Spec. Pub. London*. Magmatism in the ocean basin, **42**, 313-345.

TOMMASINI S., POLI G. & HALLIDAY A.N. (1995).- The role of sediment subduction and crustal growth in Hercynian plutonism: isotopic and trace element evidence from the Sardinia-Corsica batholith.- *J. Petrol.*, **36**, 5, 1305-1332.

VETTER P. (1968).- Géologie et paléontologie des bassins houillers de Decazeville, de Figeac et du détroit de Rodez.- Houillères du Bassin d'Aquitaine, Albi, 1-637.

WINCHESTER J.A. & FLOYD P.A (1977).- Geochemical discrimination of different magma series and their differentiation products using immobile elements.- *Chem. Geol.*, **20**, 4, 325-343.

Figure Captions

Figure 1: Schematic geologic map of the area between Lacapelle-Marival and Decazeville basins. Analysed samples are located. A: Schematic geologic map of the french Massif Central (from Basile, 2006). B: Synthetic lithostratigraphic column of the Decazeville basin (from Basile, 2006).

Figure 1: Carte géologique schématique de la région comprise entre les bassins de Lacapelle-Marival et Decazeville, avec la localisation des échantillons analysés. A: Carte géologique schématique du Massif Central français (d'après Basile, 2006). B: Colonne lithostratigraphique synthétique du bassin de Decazeville (d'après Basile, 2006).

Figure 2: Variations of minor- (TiO_2) and trace-elements (Th, U, Nb, La, Pb, Rb, Sr, Y) versus Zr. The symbols indicate the sample location (cf. Figure 1).

Figure 2: Variations des teneurs en éléments mineur (TiO_2) et traces (Th, U, Nb, La, Pb, Rb, Sr, Y) par rapport au Zr. Les symboles correspondent à la localité d'échantillonage (cf. Figure 1).

Figure 3: MgO versus SiO_2 contents (corrected for loss on ignition). Same symbols as in Figure 2. Lava terminology from MgO content (basalts for MgO > 5%, trachy-andesites for 2% < MgO < 5 %, rhyolites for MgO < 2%).

Figure 3: Variations de teneur en MgO par rapport aux teneurs en SiO_2 (corrigé de la perte au feu). Mêmes symboles que dans la Figure 2. La terminologie des laves est determinée

par la teneur en MgO (basaltes pour MgO > 5%, trachy-andésites pour 2% < MgO < 5 %, rhyolite pour MgO < 2%).

Figure 4: Zr/Ti versus Nb/Y discrimination diagram (Winchester and Floyd, 1977). Symbols indicate MgO content (cf. Figure 3).

Figure 4: Diagramme discriminant Zr/Ti par rapport à Nb/Y (Winchester and Floyd, 1977). Les symboles correspondent à la teneur en MgO (cf. Figure 3).

Figure 5: Th/Yb versus Ta/Yb discrimination diagram (Müller et al., 1992). Symbols indicate MgO content (cf. Figure 3).

Figure 5: Diagramme discriminant Th/Yb par rapport à Ta/Yb (Müller et al., 1992). Les symboles correspondent à la teneur en MgO (cf. Figure 3).

Figure 6: Chondrite-normalized rare earth elements patterns (Sun and McDonough, 1989). Sample sets as a function either of MgO content (righten column) or location (center and left). The samples are located Figure 1.

Figure 6: Spectres de terres rares normalisés aux chondrites (Sun and McDonough, 1989). Les échantillons sont regroupés soit en fonction de leur affinité magmatique (teneur en MgO, spectres de droite), soit en fonction de leur localisation (centre et gauche). Localisation des échantillons Figure 1.

Figure 7: Primitive mantle-normalized spidergrams (Sun and McDonough, 1989). Sample sets as a function either of MgO content (righten column) or location (center and left). The samples are located Figure 1.

Figure 7: Spidergrams normalisés au manteau primitif (Sun and McDonough, 1989). Les échantillons sont regroupés soit en fonction de leur affinité magmatique (teneur en MgO, spectres de droite), soit en fonction de leur localisation (centre et gauche). Localisation des échantillons Figure 1.

Figure 8: Variations of Ti/Y versus Zr/Y (left) and Nb/La versus Th/La (right). The symbols indicate either the sample location (above, cf. Figure 1) or MgO content (below, cf. Figure 3).

Figure 8 : Diagrammes Ti/Y – Zr/Y (gauche) et Nb/La – Th/La (droite). Les symboles indiquent soit la localisation des échantillons (en haut) (cf. Figure 1), soit la teneur en MgO (en bas) (cf. Figure 3).

Table Captions

Table 1: Major- and trace-element analyses, $^{87}Sr/^{86}Sr$ and $^{143}Nd/^{144}Nd$ isotope ratios for studied samples.Major oxides are in wt%, Trace-elements are in ppm. Fe_2O_3: total iron as ferric oxide; LOI: loss on ignition; bdl: below detection limit; nd: not determined. Rock types are given from MgO contents corrected for loss on ignition (Figure 3). Location Figure 1 (LM for Lacapelle-Marival).

Table 1: Analyses chimiques en éléments majeurs et traces, rapports isotopiques en $^{87}Sr/^{86}Sr$ et $^{143}Nd/^{144}Nd$ pour les échantillons étudiés. Les éléments majeurs sont donnés en %, les éléments traces en ppm. Fe_2O_3: Fer total; LOI: perte au feu; bdl: sous le seuil de detection; nd: non déterminé. La terminalogie des laves resulte des teneurs en MgO corrigées de la perte au feu (cf. Figure 3). Localisation Figure 1 (LM: Lacapelle-Marival).

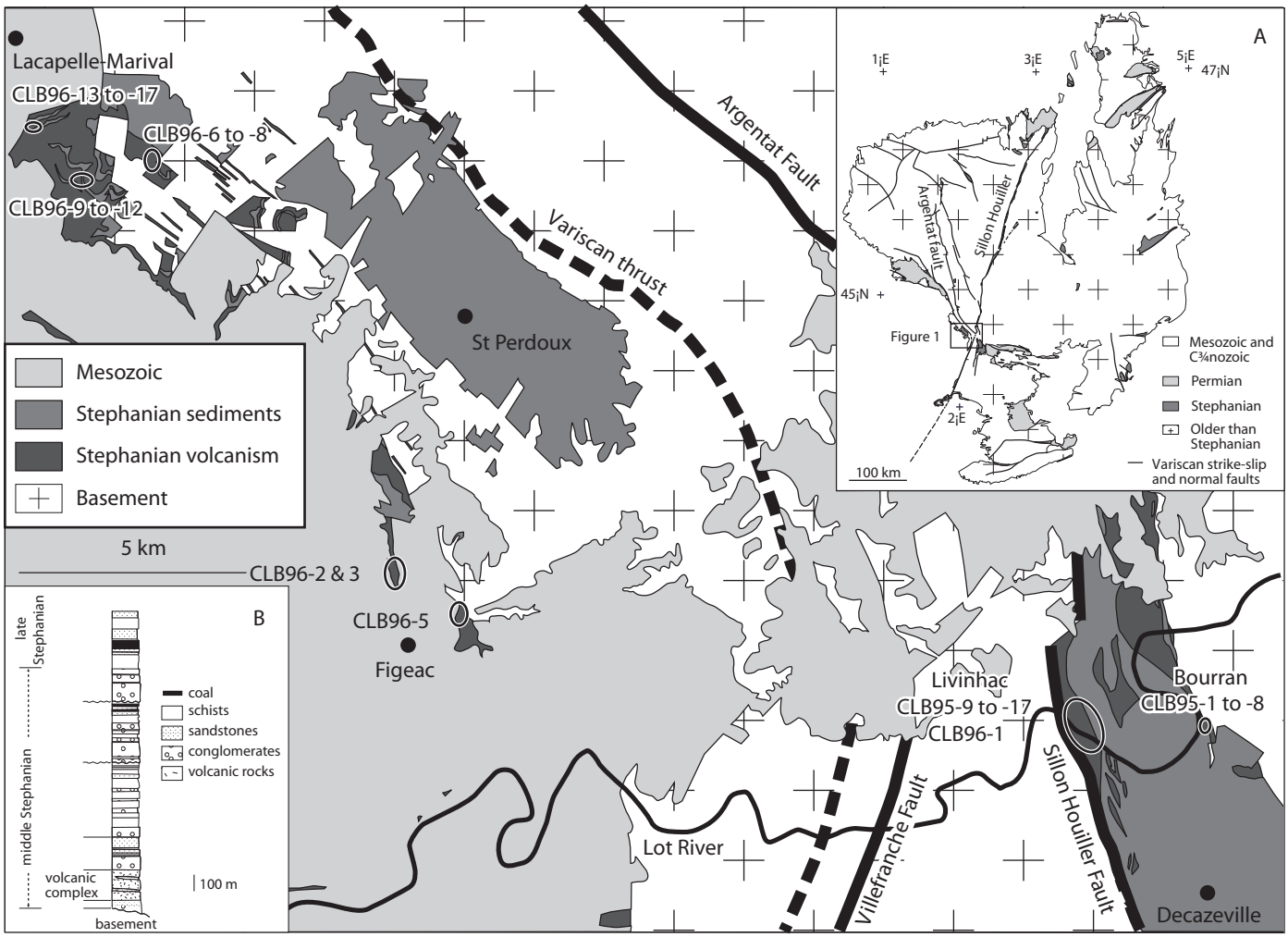
Lacapelle-Marival
CLB96-13 to -17
CLB96-6 to -8
CLB96-9 to -12
Argentat Fault
Variscan thrust
St Perdoux
Mesozoic
Stephanian sediments
Stephanian volcanism
Basement
5 km
CLB96-2 & 3
CLB96-5
Figeac
Livinhac
CLB95-9 to -17
CLB96-1
Bourran
CLB95-1 to -8
Lot River
Villefranche Fault
Sillon Houiller Fault
Decazeville
A
1¡E
3¡E
5¡E
47¡N
45¡N
2¡E
Figure 1
100 km
Mesozoic and C¾nozoic
Permian
Stephanian
Older than Stephanian
Variscan strike-slip and normal faults
B
late Stephanian
middle Stephanian
volcanic complex
basement
coal
schists
sandstones
conglomerates
volcanic rocks
100 m

Figure 2

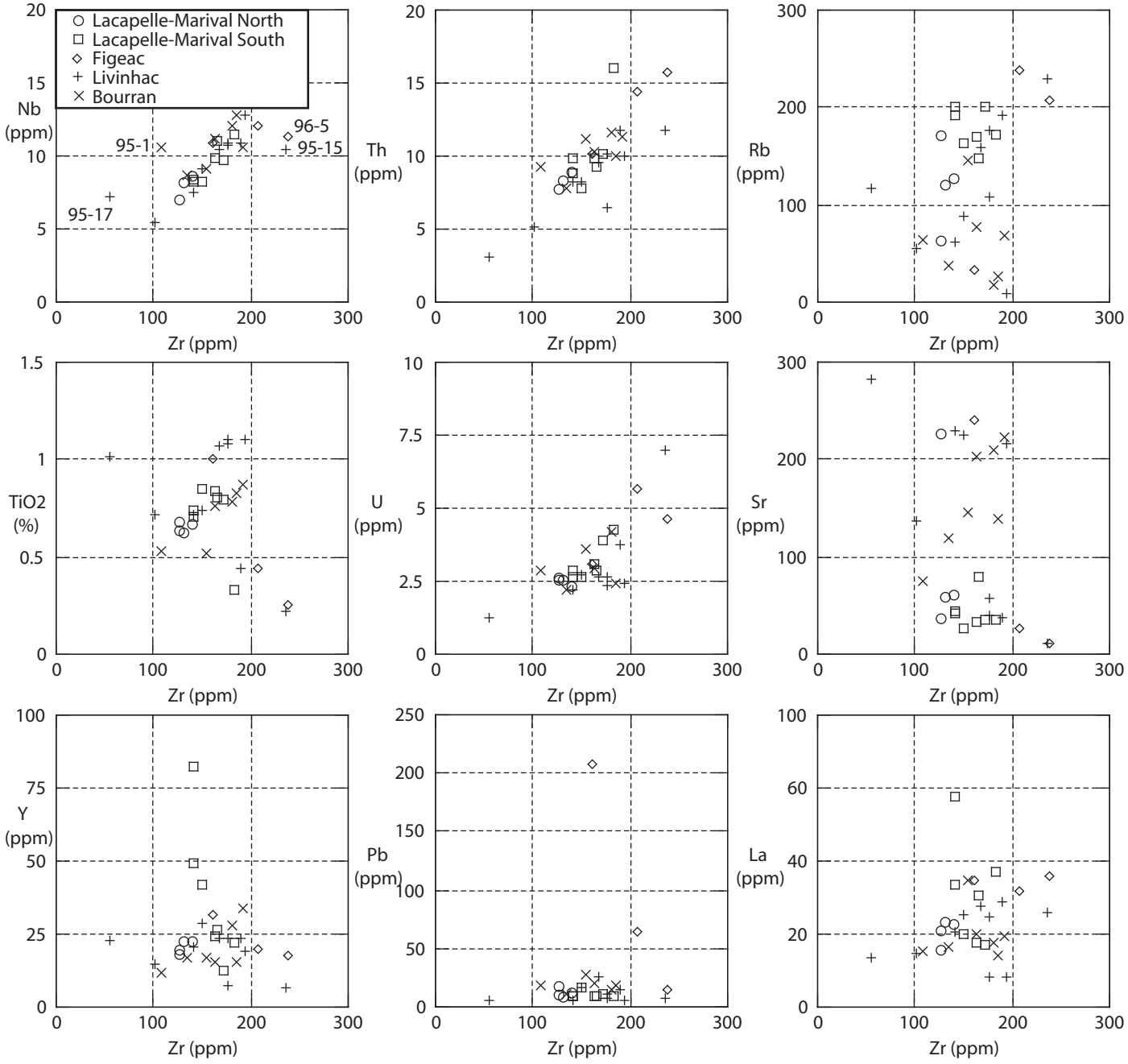
Lacapelle-Marival North
Lacapelle-Marival South
Figeac
Livinhac
Bourran
Nb (ppm)
Th (ppm)
Rb (ppm)
TiO2 (%)
U (ppm)
Sr (ppm)
Y (ppm)
Pb (ppm)
La (ppm)
Zr (ppm)
95-1
95-17
96-5
95-15

Figure 3

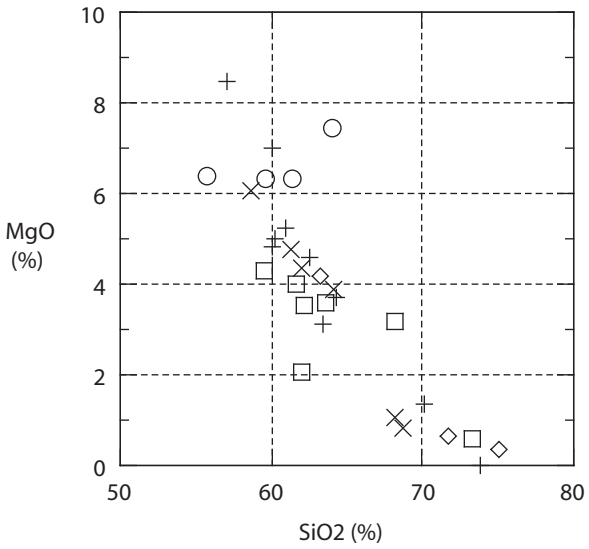

Figure 4

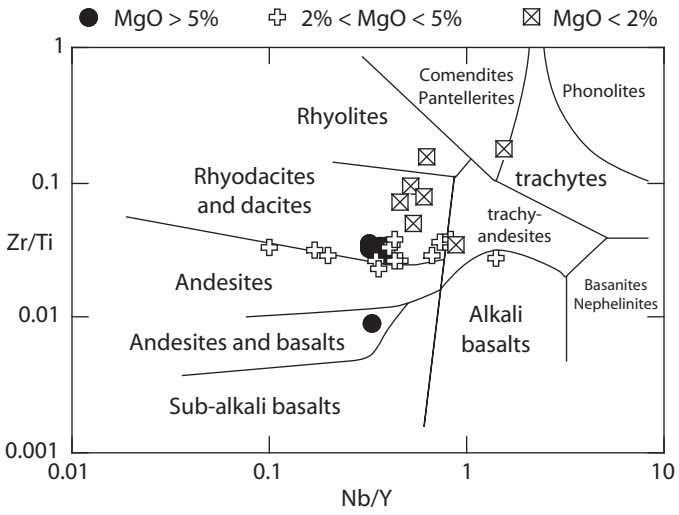
MgO > 5%
2% < MgO < 5%
MgO < 2%
1
0.1
0.01
0.001
Zr/Ti
0.01
0.1
1
10
Nb/Y
Comendites
Pantellerites
Phonolites
Rhyolites
Rhyodacites
and dacites
trachytes
trachy-
andesites
Andesites
Basanites
Nephelinites
Alkali
basalts
Andesites and basalts
Sub-alkali basalts

Figure 5

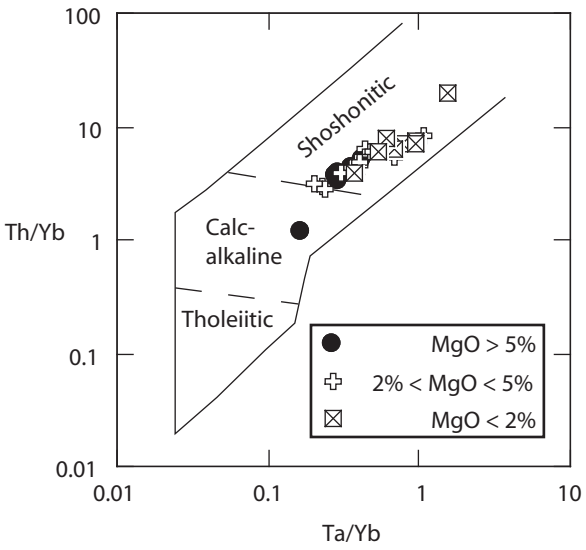
100
10
1
0.1
0.01
Th/Yb
0.01
0.1
1
10
Ta/Yb
Shoshonitic
Calc-
alkaline
Tholeiitic
MgO > 5%
2% < MgO < 5%
MgO < 2%

Figure 6

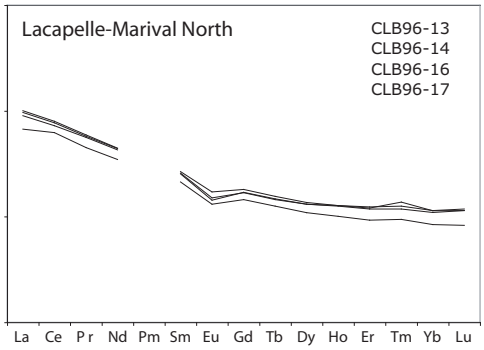
Lacapelle-Marival North
CLB96-13
CLB96-14
CLB96-16
CLB96-17
La Ce Pr Nd Pm Sm Eu Gd Tb Dy Ho Er Tm Yb Lu

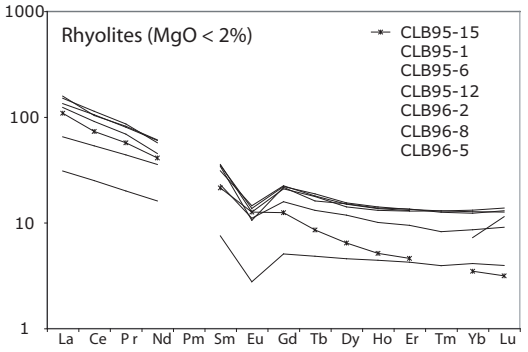
Rhyolites (MgO < 2%)
CLB95-15
CLB95-1
CLB95-6
CLB95-12
CLB96-2
CLB96-8
CLB96-5
1000
100
10
1
La Ce Pr Nd Pm Sm Eu Gd Tb Dy Ho Er Tm Yb Lu

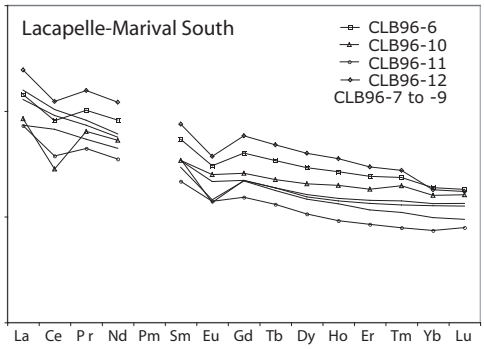
Lacapelle-Marival South
CLB96-6
CLB96-10
CLB96-11
CLB96-12
CLB96-7 to -9
La Ce Pr Nd Pm Sm Eu Gd Tb Dy Ho Er Tm Yb Lu

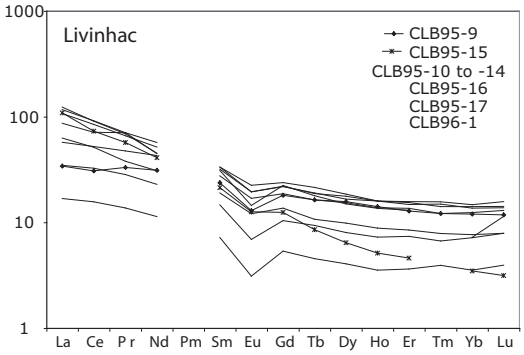
Livinhac
CLB95-9
CLB95-15
CLB95-10 to -14
CLB95-16
CLB95-17
CLB96-1
1000
100
10
1
La Ce Pr Nd Pm Sm Eu Gd Tb Dy Ho Er Tm Yb Lu

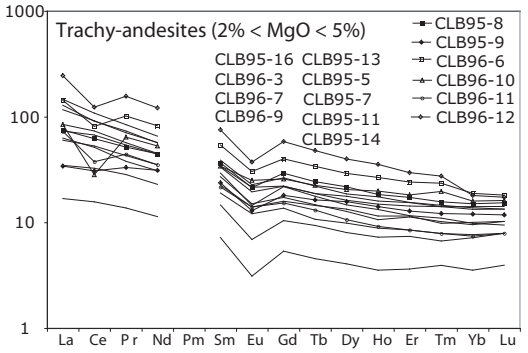
Trachy-andesites (2% < MgO < 5%)
CLB95-8
CLB95-9
CLB96-6
CLB96-10
CLB96-11
CLB96-12
CLB95-16 CLB95-13
CLB96-3 CLB95-5
CLB96-7 CLB95-7
CLB96-9 CLB95-11
CLB95-14
1000
100
10
1
La Ce Pr Nd Pm Sm Eu Gd Tb Dy Ho Er Tm Yb Lu

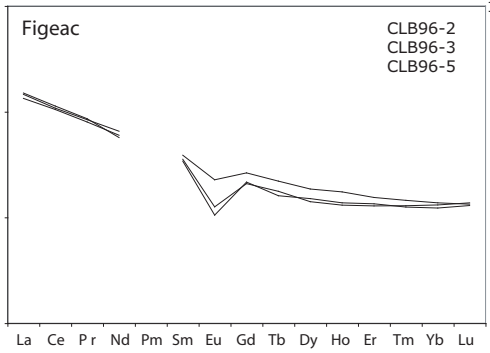
Figeac
CLB96-2
CLB96-3
CLB96-5
La Ce Pr Nd Pm Sm Eu Gd Tb Dy Ho Er Tm Yb Lu

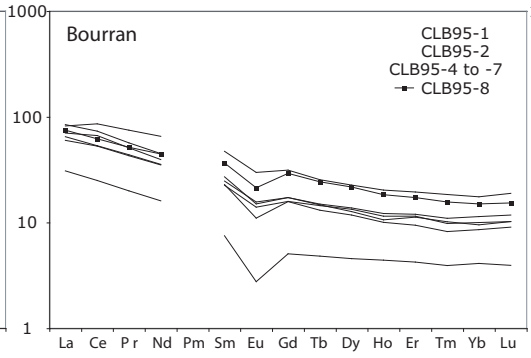
Bourran
CLB95-1
CLB95-2
CLB95-4 to -7
CLB95-8
1000
100
10
1
La Ce Pr Nd Pm Sm Eu Gd Tb Dy Ho Er Tm Yb Lu

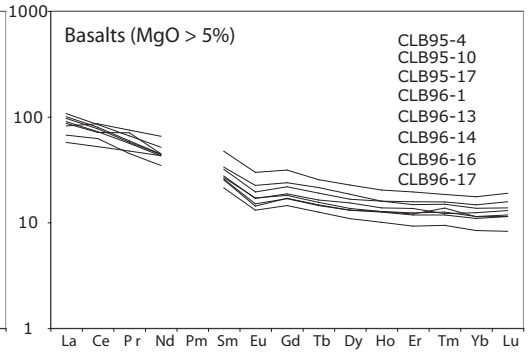
Basalts (MgO > 5%)
CLB95-4
CLB95-10
CLB95-17
CLB96-1
CLB96-13
CLB96-14
CLB96-16
CLB96-17
1000
100
10
1
La Ce Pr Nd Pm Sm Eu Gd Tb Dy Ho Er Tm Yb Lu

Figure 7

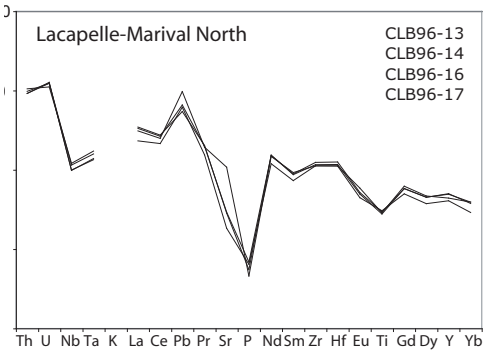
Lacapelle-Marival North
CLB96-13
CLB96-14
CLB96-16
CLB96-17
Th U Nb Ta K La Ce Pb Pr Sr P Nd Sm Zr Hf Eu Ti Gd Dy Y Yb

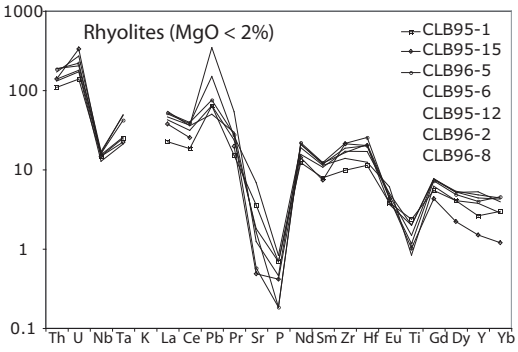
Rhyolites (MgO < 2%)
CLB95-1
CLB95-15
CLB96-5
CLB95-6
CLB95-12
CLB96-2
CLB96-8
1000
100
10
1
0.1
Th U Nb Ta K La Ce Pb Pr Sr P Nd Sm Zr Hf Eu Ti Gd Dy Y Yb

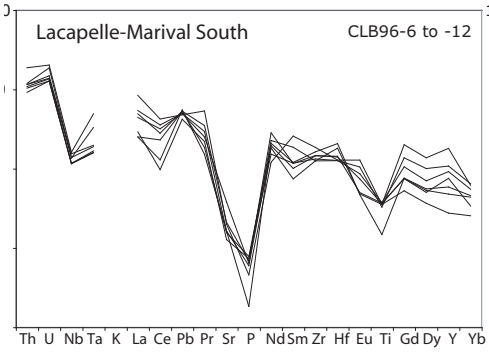
Lacapelle-Marival South
CLB96-6 to -12
Th U Nb Ta K La Ce Pb Pr Sr P Nd Sm Zr Hf Eu Ti Gd Dy Y Yb

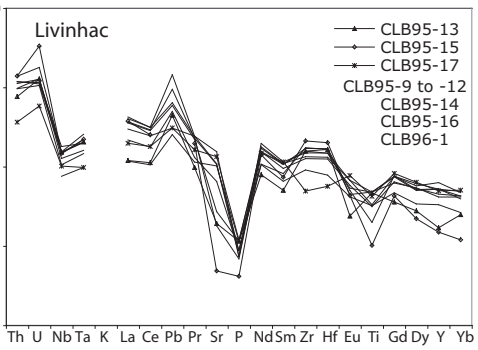
Livinhac
CLB95-13
CLB95-15
CLB95-17
CLB95-9 to -12
CLB95-14
CLB95-16
CLB96-1
1000
100
10
1
0.1
Th U Nb Ta K La Ce Pb Pr Sr P Nd Sm Zr Hf Eu Ti Gd Dy Y Yb

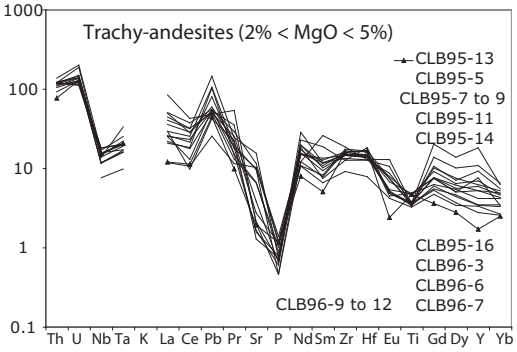
Trachy-andesites (2% < MgO < 5%)
CLB95-13
CLB95-5
CLB95-7 to 9
CLB95-11
CLB95-14
CLB95-16
CLB96-3
CLB96-6
CLB96-9 to 12
CLB96-7
1000
100
10
1
0.1
Th U Nb Ta K La Ce Pb Pr Sr P Nd Sm Zr Hf Eu Ti Gd Dy Y Yb

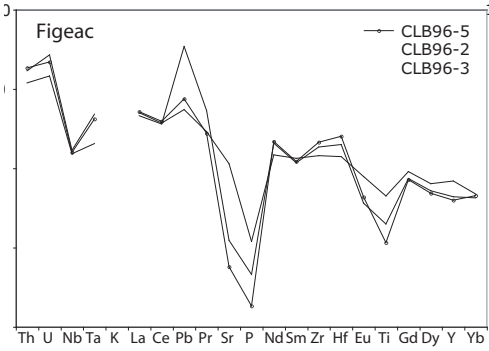
Figeac
CLB96-5
CLB96-2
CLB96-3
Th U Nb Ta K La Ce Pb Pr Sr P Nd Sm Zr Hf Eu Ti Gd Dy Y Yb

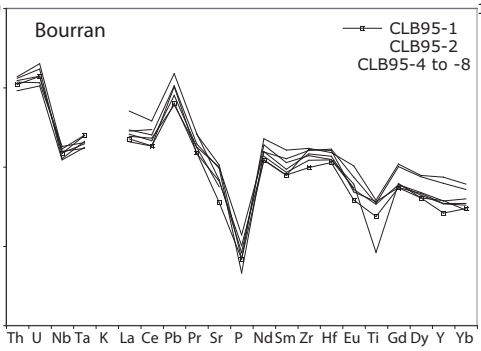
Bourran
CLB95-1
CLB95-2
CLB95-4 to -8
1000
100
10
1
0.1
Th U Nb Ta K La Ce Pb Pr Sr P Nd Sm Zr Hf Eu Ti Gd Dy Y Yb

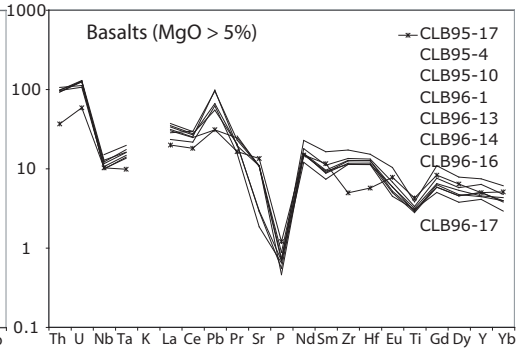
Basalts (MgO > 5%)
CLB95-17
CLB95-4
CLB95-10
CLB96-1
CLB96-13
CLB96-14
CLB96-16
CLB96-17
1000
100
10
1
0.1
Th U Nb Ta K La Ce Pb Pr Sr P Nd Sm Zr Hf Eu Ti Gd Dy Y Yb

Figure 8

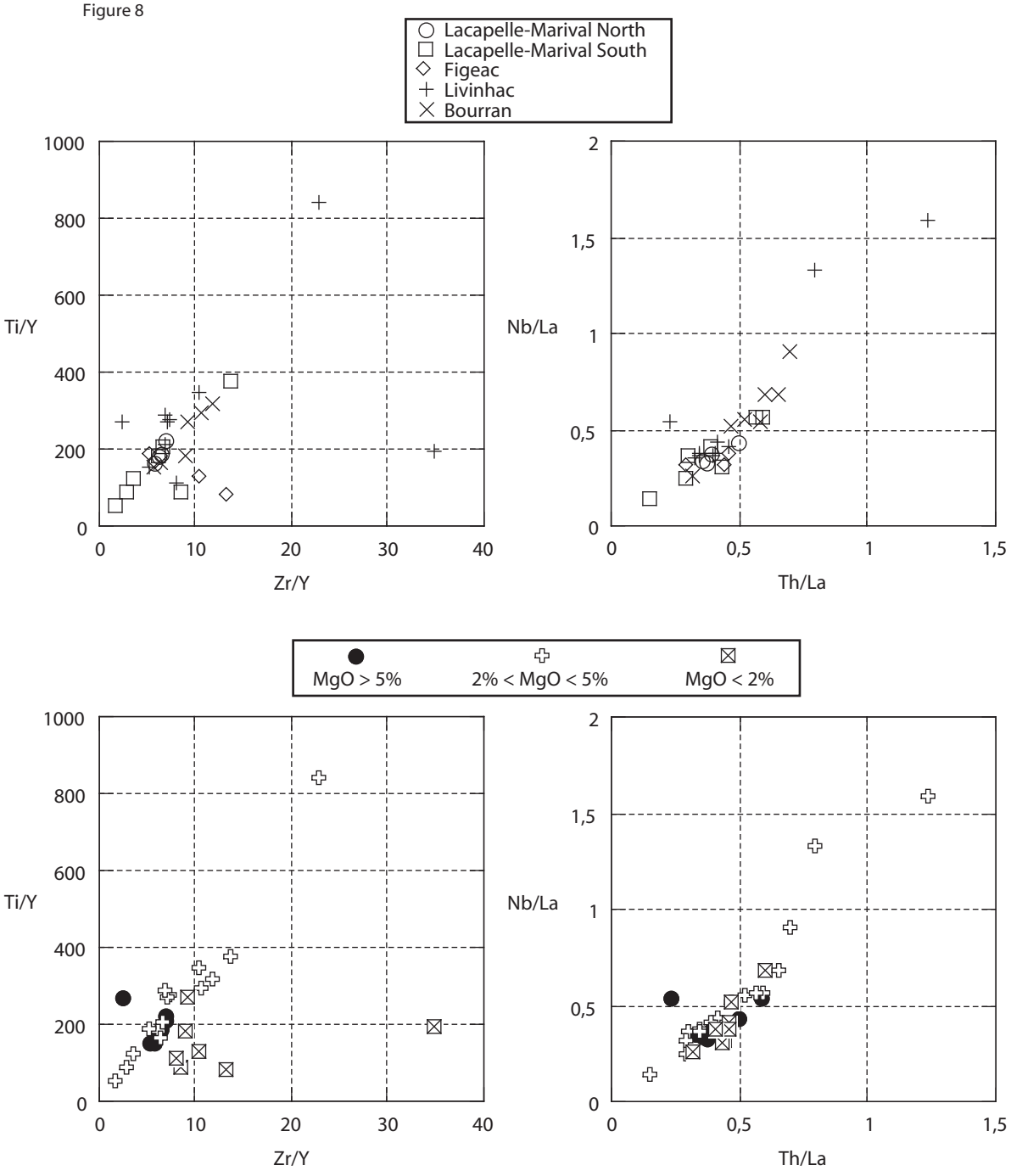
Lacapelle-Marival North
Lacapelle-Marival South
Figeac
Livinhac
Bourran
Ti/Y
Zr/Y
Nb/La
Th/La
MgO > 5%
2% < MgO < 5%
MgO < 2%